ESI: ELECTRONIC SUPPLEMENTARY INFORMATION

AN APPLIED MACHINE LEARNING FRAMEWORK FOR WASTE LITHIUM-ION BATTERY LEACHING WITH INTEGRATED PRELIMINARY ENVIRONMENTAL AND ECONOMIC ASSESSMENT

André F.M. Nogueira[1], Filipe H.B. Sosa[1], Ana C. Dias[2], João A.P. Coutinho[1], Nicolas Schaeffer[1*]

[1] CICECO – Aveiro Institute of Materials, Department of Chemistry, University of Aveiro, 3810-193 Aveiro, Portugal
[2] Centre for Environmental and Marine Studies (CESAM), Department of Environment and Planning, University of Aveiro, 3810-193 Aveiro, Portugal

*Corresponding email: nicolas.schaeffer@ua.pt

Data Sources

This work was developed using leaching data from the publications in **Table S1** and supplemented with our own unpublished data.

Table S1 – Data sources organized by year of publication

Authors	Year	Ref.
Zhang et al.	1998	[1]
Lee and Rhee	2002	[2]
Wang et al.	2009	[3]
Li et al.	2010	[4]
Li et al.	2012	[5]
Meshram et al.	2015	[6]
He et al.	2017	[7]
Gao et al.	2017	[8]
Golmohammadzadeh et al.	2017	[9]
Li et al.	2017	[10]
Chen and Ho	2018	[11]
Gao et al.	2018	[12]
Xuan et al.	2019	[13]
Chan et al.	2021	[14]
Xuan et al.	2021	[15]
Kim et al.	2022	[16]
Guimarães et al.	2022	[17]
Rouquette et al.	2023	[18]
Jiang et al.	2023	[19]
Vieceli et al.	2023	[20]
Partinen et al.	2023	[21]
Sahu and Devi	2023	[22]

Features

Table S2 – Inventory of the features and respective units organized by category

Category	Source	Feature	Unit
Reaction conditions	Manual input	inputNi	-
		inputMn	-
		inputCo	-
		Temperature	^{o}C
		Acid concentration	mol/L
		H_2O_2 concentration	wt.%
		Solid-liquid ratio	g/L
		Time	min
Basic acid descriptors	Manual input	SMILES	-
		Number of protons	-
		pKa_1	-
Dissociation constants	Manual input	pKa_2, pKa_3	-
Solubilities	Manual input	Li, Ni, Mn, Co salt solubility	g/100mL
Lipinski's rule of five	RDKit	logP	-
		TPSA	$Å^2$
		Number of HBD	-
		Number of HBA	-
		Molar weight	g/mol
Charge and polarisability	RDKit	Max partial charge	-
		Min partial charge	-
		Molar refractivity	m^3/mol
Molecular structure and functional groups	RDKit	Carboxylic acid groups	-
		C—O bonds	-
		Primary amine groups	-
		Tertiary amine groups	-
		Halogen atoms	-
		Aliphatic hydroxyl groups	-
		Sulfur atoms	-

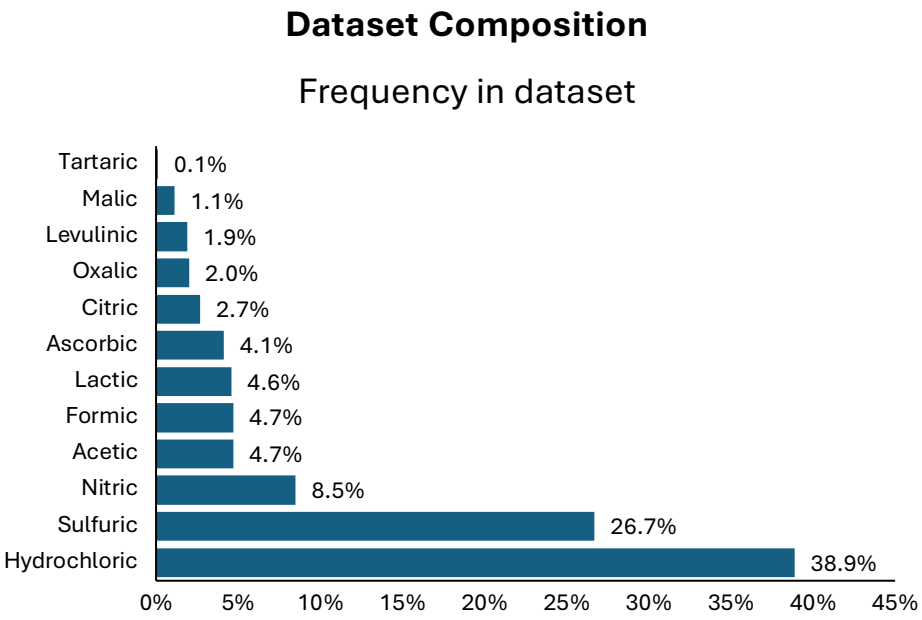

Figure S1 – Distribution of acids in the dataset

Hyperparameter optimization

Model hyperparameters were optimized using the Optuna package. [23] Optuna follows a Bayesian optimization approach to efficiently search the hyperparameter space. The parameters to optimize and the ranges to consider are specified in Table S3 of the ESI. The *Optuna* package uses Bayesian optimization to test hyperparameter combinations, considering previous optimization attempts to try to estimate the effect of varying each of the hyperparameters, resulting in a more efficient optimization than a traditional grid search, which iterates through all possible hyperparameter combinations. Each model was optimized in 20 to 100 trials. In each one, a specific hyperparameter combination is sampled from the ranges in Table S3. All parameters not mentioned were kept to the default, as implemented in the scikit-learn package. The performance of this configuration is evaluated using 5-fold cross validation, calculating the negative mean squared error (MSE) across the folds. The objective function of the optimization was to maximize the negative MSE for all models except ANN and PD-ANN, whose objective function was R^2 maximization. Optuna's MedianPruner was employed to accelerate this process, skipping unpromising trials based on intermediate results.

Table S3 – Hyperparameter optimization ranges for each of the models

Model	Hyperparameter	Range
RF	Number estimators	10 to 500
	Max depth	2 to 32 (log scale)
	Min. samples split	2 to 20
	Min. samples leaf	2 to 10
GBR	Max. iterations	50 to 500
	Max. depth	2 to 10
	Min. samples leaf	3 to 10
	Learning rate	0.01 to 0.3 (log scale)
	Max. bins	64 to 255
	L2 regularization	10^{-6} to 10 (log scale)
	Max. leaf nodes	20 to 200
ANN	Alpha	10^{-5}, 10^{-4}, 10^{-3}, 10^{-2}, 10^{-1}
	Hidden layer sizes	8, 16, 32, 64
	Activation	Logistic, ReLU, tanh
	Learning rate	Constant, adaptive
	Early stopping	True, False
PD-RF	Number estimators	100 to 500
	Max. depth	10 to 32 (log scale)
	Min. samples split	2 to 10
	Min. samples leaf	2 to 10
PD-GBR	Max. iterations	50 to 500
	Max. depth	5 to 15
	Min. samples leaf	10 to 100
	Learning rate	0.01 to 0.3 (log scale)
	Max. bins	128 to 255
	L2 regularization	10^{-6} to 10 (log scale)
	Max. leaf nodes	50 to 500
PD-ANN	Alpha	10^{-5}, 10^{-4}, 10^{-3}, 10^{-2}, 10^{-1}
	Hidden layer sizes	16, 32, 64, 128, 256
	Activation	Logistic, ReLU, tanh
	Learning rate	Constant, adaptive
	Early stopping	True, False

Performance metrics

Table S4 – Summary of the performance metrics used for model evaluation. y_i – experimental value for i-th observation; $\hat{y}_i$ – predicted value for i-th observation; $\bar{y}$ – average of the experimental values; n – number of observations.

Performance metrics	Equation
Coefficient of determination (**R^2**)	$R^2 = \frac{\sum_{i=1}^{n}(y_i - \hat{y}_i)^2}{\sum_{i=1}^{n}(y_i - \bar{y})^2}$
Mean absolute error (**MAE**)	$MAE = \frac{1}{n}\sum_{i=1}^{n}\lvert y_i - \hat{y}_i\rvert$
Median absolute error (**MedAE**)	$MedAE = median(\lvert y_i - \hat{y}_i\rvert)$
Mean squared error (**MSE**)	$MSE = \frac{1}{n}\sum_{i=1}^{n}(y_i - \hat{y}_i)^2$
Root mean squared error (**RMSE**)	$RMSE = \sqrt{\frac{1}{n}\sum_{i=1}^{n}(y_i - \hat{y}_i)^2}$

Environmental impact categories

Table S5 – Environmental impact categories and units from the Environmental Footprint 3.1 method.

Impact category	Unit
Acidification	mol H+ eq
Climate change	kg CO2 eq
Climate change - Biogenic	kg CO2 eq
Climate change - Fossil	kg CO2 eq
Climate change - Land use and LU change	kg CO2 eq
Ecotoxicity, freshwater	CTUe
Particulate matter	disease inc.
Eutrophication, marine	kg N eq
Eutrophication, freshwater	kg P eq
Eutrophication, terrestrial	mol N eq
Human toxicity, cancer	CTUh
Human toxicity, non-cancer	CTUh
Ionising radiation	kBq U-235 eq
Land use	Pt
Ozone depletion	kg CFC11 eq
Photochemical ozone formation	kg NMVOC eq
Resource use, fossils	MJ
Resource use, minerals and metals	kg Sb eq
Water use	m3 depriv.

Technical economic analysis

Table S6 – Bulk acid prices used to calculate reagent costs. A conversion rate of 1 USD to 0.88 EUR was considered.

Acid	Price (€/kg)	Purity	Location	Date	Source
Nitric	0.3934	67%	Germany	Q1 2025	ChemAnalyst [24]
Sulfuric	0.1170	98%	Germany	Q1 2025	IMARC Group [25]
Acetic	0.6160	99%	Germany	Q1 2025	ChemAnalyst [26]
Formic	0.7172	99%	Germany	Q1 2025	ChemAnalyst [27]
HCl	0.1443	36%	Germany	Q1 2025	ChemAnalyst [28]
Citric	1.2056	99%	France	Q1 2025	IMARC Group [29]
Oxalic	0.6336	98%	Germany	Q2 2024	ChemAnalyst [30]
Ascorbic	2.8600	99%	Germany	Q1 2025	IMARC Group [31]
Lactic	1.1792	90%	Germany	Q2 2024	ChemAnalyst [32]
Tartaric	1.8656	95%	Germany	Q2 2024	ChemAnalyst [33]
Malic	1.7855	99%	Netherlands	Q3 2024	ChemAnalyst [34]
Levulinic	25.2800	97%	NA	Q2 2025	Sigma-Aldrich [35]

Table S7 – Miscellaneous parameters used to calculate the heating and mixing costs of the acid slurry

Cost factor	Value	Unit	Source
Power	0.1899	€/kWh	[36]
Mixing	2.00	kW/m^3	[37]

Training set description

Table S8 – Descriptive statistics of the training set features

Feature	Min	Max	Average	Mode	Median
inputNi	0.00	0.90	0.36	0.33	0.33
inputMn	0.00	2.00	0.25	0.33	0.30
inputCo	0.00	1.00	0.40	0.33	0.33
T (°C)	20.00	95.00	58.50	50.00	60.00
pK_{a1}	-8.00	4.76	-2.89	-8.00	-3.00
pK_{a2}	0.00	11.70	1.26	0.00	0.00
pK_{a3}	0.00	6.40	0.17	0.00	0.00
Mr_{acid}	36.46	192.12	72.68	36.46	63.01
$Protons_{acid}$	1.00	3.00	1.40	1.00	1.00
[Acid] (mol/L)	0.05	8.00	2.44	1.00	2.00
$[H_2O_2]$ (wt.%)	0.00	21.00	0.71	0.00	0.00
S/L (g/L)	2.00	333.30	39.60	20.00	25.00
Time (min)	0.00	4320.00	141.60	60.00	60.00
sLi (g/100ml)	0.00	83.50	52.60	83.50	40.80
sNi (g/100ml)	0.00	94.20	46.10	66.80	44.40
sMn (g/100ml)	0.00	139.00	61.00	73.90	70.00
sCo (g/100ml)	0.00	97.40	40.40	52.90	38.00

Table S9 – Descriptive statistics of the training set targets

Target	Min	Max	Average	Mode	Median
xLi	0.00	1.00	0.78	1.00	0.84
xNi	0.00	1.00	0.64	1.00	0.66
xMn	0.00	1.00	0.58	1.00	0.55
xCo	0.00	1.00	0.57	1.00	0.52

Model selection

Table S10 – Average training statistics for each of the models. The full set of features was considered. R^2 – Coefficient of determination, MAE – mean absolute error, MedAE – median absolute error, MSE – mean square error, RMSE – root mean square error.

Model	R^2	MAE	MedAE	MSE	RMSE
RF_full	0.8878	0.0652	0.0449	0.0089	0.0943
GBR_full	0.9578	0.0371	0.0221	0.0034	0.0580
ANN_full	0.7108	0.1169	0.0892	0.0247	0.1567
PD-GBR_full	0.9966	0.0084	0.0054	0.0003	0.0165
PD-ANN_full	0.9462	0.0469	0.0357	0.0041	0.0637

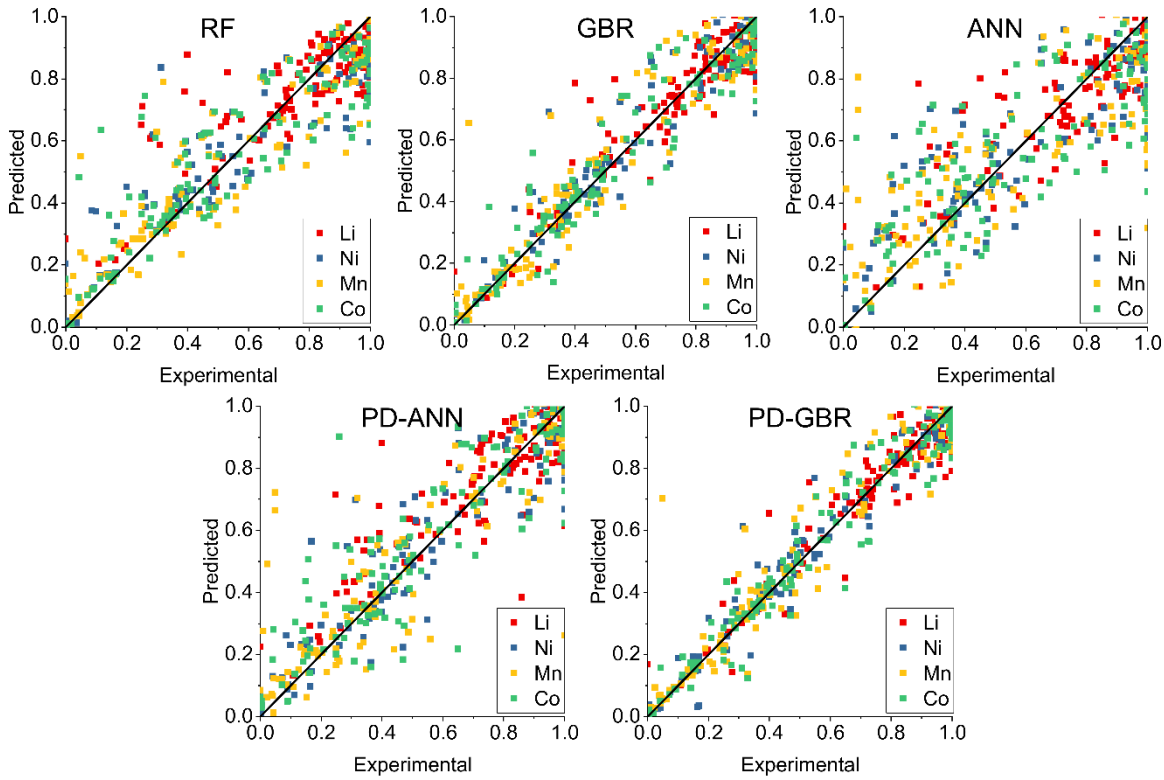

Figure S2 – Comparison of experimental yields with the predictions output by the RF, GBR, ANN, PD-ANN and PD-GBR models.

Feature selection

Table S11 – List of the model-feature pairs considered for this study and the features that each one includes. Fields marked with an asterisk (*) denote that missing values were filled in with the median value for that feature.

Model ID	Basic	pKa_2, pKa_3	Solubilities	Lipinski	Charge	Functional groups
RF_Full	X	X	X	X	X	X
GBR_full	X	X	X	X	X	X
ANN_full	X	X*	X*	X	X	X
PD-GBR_full	X	X	X	X	X	X
PD-ANN_full	X	X*	X*	X	X	X
ANN_no_pka_sol	X			X	X	X
PD-ANN_no_pka_sol	X			X	X	X
PD-GBR_base	X					
PD-GBR_pka_sol	X	X	X			
PD-GBR_no_pka	X		X	X	X	X
PD-GBR_no_sol	X	X		X	X	X
PD-GBR_no_lipinski	X	X	X		X	X
PD-GBR_no_charge_pol	X	X	X	X		X
PD-GBR_no_FG	X	X	X	X	X	

Table S12 – Training statistics for each of the model-feature set pairs. R^2 – Coefficient of determination, MAE – mean absolute error, MedAE – median absolute error, MSE – mean square error, RMSE – root mean square error.

Model	R^2	MAE	MedAE	MSE	RMSE
RF_full	0.8878	0.0652	0.0449	0.0089	0.0943
GBR_full	0.9578	0.0371	0.0221	0.0034	0.0580
ANN_full	0.7108	0.1169	0.0892	0.0247	0.1567
PD-GBR_full	0.9966	0.0084	0.0054	0.0003	0.0165
PD-ANN_full	0.9462	0.0469	0.0357	0.0041	0.0637
ANN_no_pKa_sol	0.7432	0.1088	0.0824	0.0212	0.1457
PD-ANN_no_pKa_sol	0.9677	0.0362	0.0261	0.0026	0.0508
PD-GBR_base	0.9898	0.0192	0.0132	0.0009	0.0293
PD_GBR_pKa_sol	0.9970	0.0072	0.0046	0.0002	0.0155
PD-GBR_no_pKa	0.9951	0.0121	0.0083	0.0004	0.0201
PD-GBR_no_sol	0.9727	0.0338	0.0243	0.0023	0.0479
PD-GBR_no_lipinski	0.9915	0.0172	0.0117	0.0007	0.0266
PD-GBR_no_charge_pol	0.9964	0.0091	0.0060	0.0003	0.0171
PD-GBR_no_FG	0.9965	0.0083	0.0052	0.0003	0.0167

Table S13 – Test statistics for each of the model-feature set pairs. R2 – Coefficient of determination, MAE – mean absolute error, MedAE – median absolute error, MSE – mean square error, RMSE – root mean square error.

Model	R^2	MAE	MedAE	MSE	RMSE
RF_full	0.8026	0.0963	0.0741	0.0181	0.1344
GBR_full	0.9137	0.0617	0.0411	0.0081	0.0896
ANN_full	0.6840	0.1319	0.1036	0.0306	0.1737
PD-GBR_full	**0.9332**	0.0513	0.0283	0.0063	0.0787
PD-ANN_full	0.8044	0.0933	0.0636	0.0180	0.1336
ANN_no_pKa_sol	0.6922	0.1275	0.0977	0.0289	0.1696
PD-ANN_no_pKa_sol	0.7978	0.0928	0.0621	0.0190	0.1373
PD_GBR_base	0.9222	0.0566	0.0341	0.0072	0.0847
PD_GBR_pKa_sol	0.9282	0.0527	0.0274	0.0066	0.0811
PD-GBR_no_pKa	0.9265	0.0527	0.0281	0.0068	0.0824
PD-GBR_no_sol	0.9226	0.0605	0.0447	0.0073	0.0851
PD-GBR_no_lipinski	**0.9296**	0.0541	0.0330	0.0067	0.0817
PD-GBR_no_charge_pol	**0.9297**	0.0528	0.0303	0.0067	0.0810
PD-GBR_no_FG	0.9269	0.0531	0.0298	0.0069	0.0826

Model analysis

Table S14 – Pairwise comparison of MAE of HCl, Sulfuric, Nitric and the remaining acid systems. Each row tests the null hypothesis that the distribution of MAE is the same in both samples.

Samples	Test Stat.	Std. Error	Std. Test Stat.	Sig.	Adj. Sig.
Other – HCl	49.752	16.599	2.997	0.003	0.016
Other – Sulfuric	-56.005	17.843	-3.139	0.002	0.010
Other – Nitric	97.402	26.628	3.658	< 0.001	0.002
HCl – Sulfuric	-6.253	17.758	-0.352	0.725	1.000
HCl – Nitric	-47.650	26.572	-1.793	0.073	0.438
Sulfuric – Nitric	41.397	27.365	1.513	0.130	0.782

Table S15 – Two-tailed significance (p-values) from Wilcoxon signed-rank tests comparing the MAE of the base feature set versus the full feature set for each acid group.

Acid	p-value
HCl	0.066
Sulfuric	0.932
Nitric	0.995
Other	0.016

Table S16 – Pairwise comparison of MAE of low (< 0.3), middling (between 0.3 and 0.7) and high (> 0.7) yield systems. Each row tests the null hypothesis that the distribution of MAE is the same in both samples.

Samples	Test Stat.	Std. Error	Std. Test Stat.	Sig.	Adj. Sig.
y<0.3 – y>0.7	-48.664	17.996	-2.704	0.007	0.021
y<0.3 – 0.3<y<0.7	73.846	19.749	3.739	<.001	0.001
y>0.7 – 0.3<y<0.7	25.182	15.661	1.608	0.108	0.324

Table S17 – Pairwise comparison of MAE of prediction for systems containing different cathode chemistries. Each row tests the null hypothesis that the distribution of MAE is the same in both samples.

Samples	Test Stat.	Std. Error	Std. Test Stat.	Sig.	Adj. Sig.
NMC811 – NMC333	54.009	20.972	2.575	0.010	0.060
NMC811 – Other	-57.903	21.590	-2.682	0.007	0.044
NMC811 – NMC622	159.670	27.345	5.839	<.001	0.000
NMC333 – Other	-3.894	15.691	-0.248	0.804	1.000
NMC333 – NMC622	-105.661	22.974	-4.599	<.001	0.000
Other – NMC622	101.767	23.539	4.323	<.001	0.000

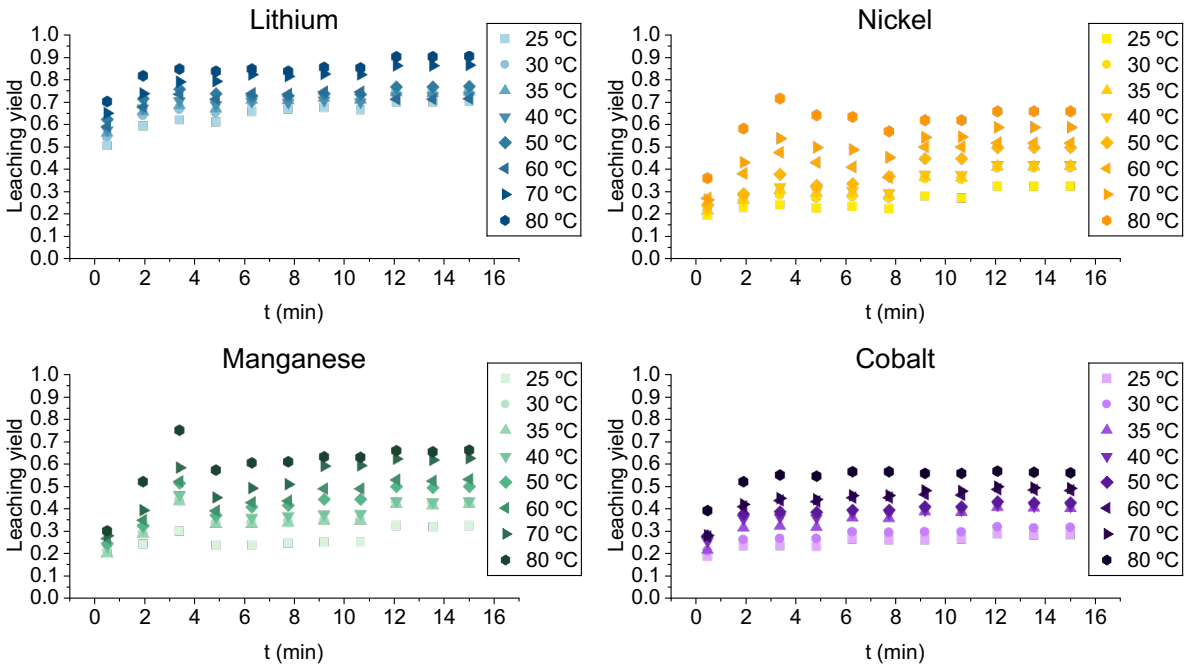

Figure S3 – Kinetics curves produced by the PD-GBR model for activation energy calculation

Table S18 – Coefficients of determination (R2) for four kinetic models fitted to the leaching data of Li, Ni, Mn, and Co using 2 M HCl, 50 g/L at 25 °C.

Model	Li	Ni	Mn	Co
Linear	0.8049	0.8563	0.8229	0.8207
SCM (chemical reaction control)	0.8292	0.8668	0.8300	0.8277
SCM (product layer diffusion control)	0.8794	0.9339	0.8714	0.8863
SCM (film diffusion and chemical reaction control)	0.9173	0.9420	0.8753	0.8963

References

[1] P. Zhang, T. Yokoyama, O. Itabashi, T.M. Suzuki, K. Inoue, Hydrometallurgical process for recovery of metal values from spent lithium-ion secondary batteries, Hydrometallurgy 47 (1998) 259–271. https://doi.org/10.1016/S0304-386X(97)00050-9.

[2] C.K. Lee, K.-I. Rhee, Preparation of LiCoO2 from spent lithium-ion batteries, Journal of Power Sources 109 (2002) 17–21. https://doi.org/10.1016/S0378-7753(02)00037-X.

[3] R.-C. Wang, Y.-C. Lin, S.-H. Wu, A novel recovery process of metal values from the cathode active materials of the lithium-ion secondary batteries, Hydrometallurgy 99 (2009) 194–201. https://doi.org/10.1016/j.hydromet.2009.08.005.

[4] L. Li, J. Ge, F. Wu, R. Chen, S. Chen, B. Wu, Recovery of cobalt and lithium from spent lithium ion batteries using organic citric acid as leachant, Journal of Hazardous Materials 176 (2010) 288–293. https://doi.org/10.1016/j.jhazmat.2009.11.026.

[5] L. Li, J. Lu, Y. Ren, X.X. Zhang, R.J. Chen, F. Wu, K. Amine, Ascorbic-acid-assisted recovery of cobalt and lithium from spent Li-ion batteries, Journal of Power Sources 218 (2012) 21–27. https://doi.org/10.1016/j.jpowsour.2012.06.068.

[6] P. Meshram, B.D. Pandey, T.R. Mankhand, Recovery of valuable metals from cathodic active material of spent lithium ion batteries: Leaching and kinetic aspects, Waste Management 45 (2015) 306–313. https://doi.org/10.1016/j.wasman.2015.05.027.

[7] L.-P. He, S.-Y. Sun, X.-F. Song, J.-G. Yu, Leaching process for recovering valuable metals from the LiNi 1/3 Co 1/3 Mn 1/3 O 2 cathode of lithium-ion batteries, Waste Management 64 (2017) 171–181. https://doi.org/10.1016/j.wasman.2017.02.011.

[8] W. Gao, X. Zhang, X. Zheng, X. Lin, H. Cao, Y. Zhang, Z. Sun, Lithium Carbonate Recovery from Cathode Scrap of Spent Lithium-Ion Battery: A Closed-Loop Process, Environ. Sci. Technol. 51 (2017) 1662–1669. https://doi.org/10.1021/acs.est.6b03320.

[9] R. Golmohammadzadeh, F. Rashchi, E. Vahidi, Recovery of lithium and cobalt from spent lithium-ion batteries using organic acids: Process optimization and kinetic aspects, Waste Management 64 (2017) 244–254. https://doi.org/10.1016/j.wasman.2017.03.037.

[10] L. Li, E. Fan, Y. Guan, X. Zhang, Q. Xue, L. Wei, F. Wu, R. Chen, Sustainable Recovery of Cathode Materials from Spent Lithium-Ion Batteries Using Lactic Acid Leaching System, ACS Sustainable Chem. Eng. 5 (2017) 5224–5233. https://doi.org/10.1021/acssuschemeng.7b00571.

[11] W.-S. Chen, H.-J. Ho, Recovery of Valuable Metals from Lithium-Ion Batteries NMC Cathode Waste Materials by Hydrometallurgical Methods, Metals 8 (2018) 321. https://doi.org/10.3390/met8050321.

[12] W. Gao, J. Song, H. Cao, X. Lin, X. Zhang, X. Zheng, Y. Zhang, Z. Sun, Selective recovery of valuable metals from spent lithium-ion batteries – Process development and kinetics evaluation, Journal of Cleaner Production 178 (2018) 833–845. https://doi.org/10.1016/j.jclepro.2018.01.040.

[13] W. Xuan, A. Otsuki, A. Chagnes, Investigation of the leaching mechanism of NMC 811 (LiNi0.8Mn0.1Co0.1O2) by hydrochloric acid for recycling lithium ion battery cathodes, RSC Adv. 9 (2019) 38612–38618. https://doi.org/10.1039/C9RA06686A.

[14] K.H. Chan, J. Anawati, M. Malik, G. Azimi, Closed-Loop Recycling of Lithium, Cobalt, Nickel, and Manganese from Waste Lithium-Ion Batteries of Electric Vehicles, ACS Sustainable Chem. Eng. 9 (2021) 4398–4410. https://doi.org/10.1021/acssuschemeng.0c06869.

[15] W. Xuan, A. de Souza Braga, C. Korbel, A. Chagnes, New insights in the leaching kinetics of cathodic materials in acidic chloride media for lithium-ion battery recycling, Hydrometallurgy 204 (2021) 105705. https://doi.org/10.1016/j.hydromet.2021.105705.

[16] E. Kim, T. Ahn, T.-Y. Kim, New method for selective recovery of manganese from NCM-based cathode material of spent Li-ion batteries, Geosystem Engineering 25 (2022) 143–149. https://doi.org/10.1080/12269328.2022.2119610.

[17] L.F. Guimarães, A.B. Botelho Junior, D.C.R. Espinosa, Sulfuric acid leaching of metals from waste Li-ion batteries without using reducing agent, Minerals Engineering 183 (2022) 107597. https://doi.org/10.1016/j.mineng.2022.107597.
[18] L.M.J. Rouquette, M. Petranikova, N. Vieceli, Complete and selective recovery of lithium from EV lithium-ion batteries: Modeling and optimization using oxalic acid as a leaching agent, Separation and Purification Technology 320 (2023) 124143. https://doi.org/10.1016/j.seppur.2023.124143.
[19] T. Jiang, Q. Shi, Z. Wei, K. Shah, H. Efstathiadis, X. Meng, Y. Liang, Leaching of valuable metals from cathode active materials in spent lithium-ion batteries by levulinic acid and biological approaches, HELIYON 9 (2023). https://doi.org/10.1016/j.heliyon.2023.e15788.
[20] N. Vieceli, P. Benjamasutin, R. Promphan, P. Hellström, M. Paulsson, M. Petranikova, Recycling of Lithium-Ion Batteries: Effect of Hydrogen Peroxide and a Dosing Method on the Leaching of LCO, NMC Oxides, and Industrial Black Mass, ACS Sustainable Chem. Eng. 11 (2023) 9662–9673. https://doi.org/10.1021/acssuschemeng.3c01238.
[21] J. Partinen, P. Halli, B.P. Wilson, M. Lundström, The impact of chlorides on NMC leaching in hydrometallurgical battery recycling, Minerals Engineering 202 (2023) 108244. https://doi.org/10.1016/j.mineng.2023.108244.
[22] S. Sahu, N. Devi, Two-step leaching of spent lithium-ion batteries and effective regeneration of critical metals and graphitic carbon employing hexuronic acid, RSC Adv. 13 (2023) 7193–7205. https://doi.org/10.1039/D2RA07926G.
[23] T. Akiba, S. Sano, T. Yanase, T. Ohta, M. Koyama, Optuna: A Next-generation Hyperparameter Optimization Framework, in: Proceedings of the 25th ACM SIGKDD International Conference on Knowledge Discovery & Data Mining, Association for Computing Machinery, New York, NY, USA, 2019: pp. 2623–2631. https://doi.org/10.1145/3292500.3330701.
[24] ChemAnalyst, Nitric Acid Prices, News, Monitor, Market Analysis & Demand, (n.d.). https://www.chemanalyst.com/Pricing-data/nitric-acid-1142 (accessed June 26, 2025).
[25] IMARC Group, Sulfuric Acid Price Index, Chart and Trend 2025, (n.d.). https://www.imarcgroup.com/sulfuric-acid-pricing-report (accessed June 26, 2025).
[26] ChemAnalyst, Acetic Acid Prices, News, Monitor, Analysis & Demand, (n.d.). https://www.chemanalyst.com/Pricing-data/acetic-acid-9 (accessed June 26, 2025).
[27] ChemAnalyst, Formic Acid Prices, News, Monitor, Market Analysis & Demand, (n.d.). https://www.chemanalyst.com/Pricing-data/formic-acid-1242 (accessed June 26, 2025).
[28] ChemAnalyst, Hydrochloric Acid Prices, Monitor, Market Analysis & Demand, (n.d.). https://www.chemanalyst.com/Pricing-data/hydrochloric-acid-61 (accessed June 26, 2025).
[29] IMARC Group, Citric Acid Prices, Chart, News, Demand and Forecast, (n.d.). https://www.imarcgroup.com/citric-acid-pricing-report (accessed June 26, 2025).
[30] Oxalic Acid Prices, News, Monitor, Analysis & Demand, (n.d.). https://www.chemanalyst.com/Pricing-data/oxalic-acid-1556 (accessed June 27, 2025).
[31] IMARC Group, Ascorbic Acid Price Trend, Index and Chart 2025, (n.d.). https://www.imarcgroup.com/ascorbic-acid-pricing-report (accessed June 26, 2025).
[32] ChemAnalyst, Lactic Acid Prices, News, Monitor, Analysis & Demand, (n.d.). https://www.chemanalyst.com/Pricing-data/lactic-acid-1435 (accessed June 26, 2025).
[33] ChemAnalyst, Tartaric Acid Prices, News, Monitor, Analysis & Demand, (n.d.). https://www.chemanalyst.com/Pricing-data/tartaric-acid-1126 (accessed June 26, 2025).
[34] ChemAnalyst, Malic Acid Prices, News, Monitor, Analysis & Demand, (n.d.). https://www.chemanalyst.com/Pricing-data/malic-acid-1281 (accessed June 26, 2025).

[35] Sigma-Aldrich, Levulinic acid = 97 , FG 123-76-2, (n.d.). https://www.sigmaaldrich.com/PT/en/product/aldrich/w262706 (accessed June 26, 2025).
[36] Eurostat, Electricity prices for non-household consumers - bi-annual data (from 2007 onwards), (2022). https://doi.org/10.2908/NRG_PC_205.
[37] R.K. Sinnott, Coulson & Richardson's Chemical Engineering, 4th ed, Elsevier Butterworth-Heinemann, Amsterdam Paris, 2005.